



OPEN

# *Pm*AP2- $\beta$ depletion enhanced activation of the Toll signaling pathway during yellow head virus infection in the black tiger shrimp *Penaeus monodon*

Thapanan Jatuyosporn<sup>1,2</sup>, Pasunee Laohawutthichai<sup>1,2</sup>, Premruethai Supungul<sup>3</sup>, Rogerio R. Sotelo-Mundo<sup>4</sup>, Adrian Ochoa-Leyva<sup>5</sup>, Anchalee Tassanakajon<sup>2</sup> & Kuakarun Krusong<sup>1</sup>✉

Yellow head virus (YHV) is a pathogen which causes high mortality in penaeid shrimp. Previous studies suggested that YHV enters shrimp cells via clathrin-mediated endocytosis. This research investigated the roles of clathrin adaptor protein 2 subunit  $\beta$  (AP-2 $\beta$ ) from *Penaeus monodon* during YHV infection. *Pm*AP2- $\beta$  was continuously up-regulated more than twofold during 6–36 hpi. Suppression of *Pm*AP2- $\beta$  significantly reduced YHV copy numbers and delayed shrimp mortality. Quantitative RT-PCR revealed that knockdown of *Pm*AP2- $\beta$  significantly enhanced the expression level of *Pm*Spätzle, a signaling ligand in the Toll pathway, by 30-fold at 6 and 12 hpi. Moreover, the expression levels of gene components in the Imd and JAK/STAT signaling pathways under the suppression of *Pm*AP2- $\beta$  during YHV infection were also investigated. Interestingly, anti-lipopolysaccharide factor isoform 3 (ALFPm3) was up-regulated by 40-fold in *Pm*AP2- $\beta$  knockdown shrimp upon YHV infection. In addition, silencing of *Pm*AP2- $\beta$  dramatically enhanced crustin*Pm*1 expression in YHV-infected shrimp. Knockdown of ALFPm3 and crustin*Pm*1 significantly reduced shrimp survival rate. Taken together, this work suggested that *Pm*AP2- $\beta$ -deficiency promoted the Toll pathway signalings, resulting in elevated levels of ALFPm3 and crustin*Pm*1, the crucial antimicrobial peptides in defence against YHV.

## Abbreviations

ALFs	Anti-lipopolysaccharide factors
AMPs	Antimicrobial peptides
Imd	Immune deficiency
<i>Pm</i>	<i>Penaeus monodon</i>
WSSV	White spot syndrome virus
YHV	Yellow head virus

Yellow head virus (YHV) is a lethal positive-sense single-stranded RNA virus with a spike envelope. YHV widely infects penaeid shrimps, including *Euphausia superba*, *Litopenaeus setiferus*, *P. merguensis*, *Metapenaeus ensis*, *L. vannamei*, *P. stylirostris*, *P. setiferus*, *P. aztecus* and *P. duorarum*<sup>1–3</sup>. YHV entry via the clathrin-mediated endocytosis has been identified by endocytosis inhibition and by silencing of the clathrin coated assembly protein

<sup>1</sup>Structural and Computational Biology Research Unit, Department of Biochemistry, Faculty of Science, Chulalongkorn University, Bangkok 10330, Thailand. <sup>2</sup>Center of Excellence for Molecular Biology and Genomics of Shrimp, Department of Biochemistry, Faculty of Science, Chulalongkorn University, Bangkok 10330, Thailand. <sup>3</sup>National Center for Genetic Engineering and Biotechnology (BIOTEC), National Science and Technology Development Agency (NSTDA), Pathumthani 12120, Thailand. <sup>4</sup>Laboratorio de Estructura Biomolecular, Centro de Investigación en Alimentación Y Desarrollo, A.C. (CIAD), Carretera Gustavo Enrique Astiazaran Rosas No. 46, 83304 Hermosillo, Sonora, Mexico. <sup>5</sup>Departamentos de Microbiología Molecular, Universidad Nacional Autónoma de México (UNAM), Avenida Universidad 2001, Colonia Chamilpa, 62210 Cuernavaca, Mexico. ✉email: Kuakarun.K@chula.ac.th

17 (AP17), a  $\sigma 2$  subunit of the adaptor protein complex, and clathrin heavy chain<sup>4,5</sup>. Suppression of *PmRab7*, a transportation protein involving in late endosome trafficking, resulted in a decrease in YHV<sup>6</sup>.

In general, clathrin-mediated endocytosis is a well-characterized endocytic mechanism for uptaking nutrients, pathogens antigens, growth factors and receptors. Initiation of the clathrin-mediated endocytosis requires the accumulation of phosphatidylinositol-4,5-bisphosphate (PIP2) and clathrin assembly protein 2 (AP2) complex at the plasma membrane. AP2 consists of 4 subunits, including  $\beta 2$ ,  $\alpha$ ,  $\mu 2$  and  $\sigma 2$ . In *P. monodon*, the  $\beta 2$ ,  $\mu 2$  and  $\sigma 2$  subunits of AP-2 have been characterized<sup>4,7</sup>.

AP2 complex first binds to the cytoplasmic tail of the ligand-receptor complex and recruits other accessory proteins such as clathrin, epsin and  $\beta$ -arrestin to form clathrin-coated pits, which are then pitched off from the plasma membrane by GTPase dynamin<sup>8</sup>. The endocytic vesicle then fuses with the early endosome from where the ligand-receptor is sorted by either for recycling via Rab4- or Rab11-dependent pathway or for degradation in lysosomes via Rab7<sup>9</sup>. Several viruses, including semliki forest virus<sup>10</sup>, vesicular stomatitis virus<sup>11</sup>, influenza A virus<sup>12</sup>, Foot- and mouth disease virus<sup>13</sup> and hepatitis C<sup>14</sup>, hijack the clathrin-mediated endocytosis to enter host cells. Previously, the white spot syndrome virus (WSSV), the most devastating pathogen in shrimp, was also reported to invade host cells via clathrin-dependent endocytic route<sup>7,15,16</sup>.

Clathrin-mediated endocytosis is responsible for transporting a wide variety of cargoes from the plasma membrane into the cell. This process does not only maintain membrane compositions but also controls cell-signaling pathways. The internalized ligand-receptor complex remains signal transduction as they are located at plasma membrane<sup>17</sup>. Intervention of endocytosis may disrupt intracellular signaling networks, leading to malfunctioning in many cellular processes such as cell development, migration and neuroplasticity<sup>18,19</sup>. In *Drosophila*, endosomal entry regulates Notch receptor activation<sup>20</sup> and the endocytic mechanism also controls the JAK/STAT (Janus tyrosine kinase/Signal transducer and activator of transcription) signaling<sup>21</sup>. In HeLaM cells, clathrin-mediated endocytosis of type-I interferon (IFN- $\alpha/\beta$ ) receptor (IFNAR) is required for the activation of JAK/STAT signaling and the activities of type-I IFNs<sup>22</sup>. Clathrin controls Wnt/ $\beta$ -catenin signaling by manipulating exocytosis of transmembrane proteins such as cadherins and Wnt co-receptors<sup>23</sup>. Lipopolysaccharide (LPS) receptor is mediated by clathrin and colocalized with the Toll-like receptor, TLR4, on early/sorting endosomes<sup>24</sup>. The disruption of endocytosis and endosomal sorting results in increased LPS signaling. In addition, the impairment of clathrin internalization enhances expression of lymphotoxin  $\beta$  receptor (LT $\beta$ R) and activation of canonical NF- $\kappa$ B signaling<sup>25</sup>. These evidences suggest that clathrin-dependent endocytosis could regulate several signaling pathways.

In shrimp, antimicrobial peptides play an important role in defence against viral and bacterial infections. The expression of antimicrobial peptides was controlled by different signaling pathways. The Toll and Immune Deficiency (Imd) signaling pathways are one of the first lines of shrimp innate immunity. Previously, ALFPm3 was reported to have been governed by the Toll and the Imd pathways<sup>26</sup>. CrustinPm1 was regulated by the Toll signaling pathway while crustinPm7 was mediated through both Toll and Imd pathways<sup>27</sup>. Expression of PEN3 was under the regulation of both Toll and Imd pathways, while PEN5 was controlled by the Imd<sup>28</sup>.

In this study, RNA interference techniques, immunofluorescence confocal microscopy, transmission electron microscopy (TEM) and mortality study were employed to investigate the roles of *PmAP2- $\beta$*  during YHV infection. The transcription levels of genes in the Toll, Imd and JAK/STAT signaling pathways and other immune response genes were examined under the suppression of *PmAP2- $\beta$*  during YHV challenge. This work reveals the roles of clathrin-mediated endocytosis during YHV infection.

## Results

**Influence of *PmAP2- $\beta$*  during YHV infection.** To investigate the function of *PmAP2- $\beta$*  during YHV infection, shrimp hemocytes were collected at different timepoints after YHV injection to measure the transcription level of *PmAP2- $\beta$* . Based on quantitative RT-PCR analysis, *PmAP2- $\beta$*  was constantly up-regulated more than twofold in all observed timepoints (Fig. 1A). Immunofluorescence confocal microscopy confirmed that *PmAP2- $\beta$*  was highly expressed at protein level upon YHV infection (Fig. 1B). Silencing of *PmAP2- $\beta$*  delayed the cumulative mortality caused by YHV (Fig. 1C) and also reduced YHV copy numbers (Fig. 1D). This suggested that *PmAP2- $\beta$*  knockdown interfered with YHV propagation.

**Localization of *PmAP2- $\beta$*  during YHV infection.** *PmAP2- $\beta$*  was probed by a 10-nm gold particle conjugated with *PmAP2- $\beta$*  antibody in order to visualize *PmAP2- $\beta$*  during YHV infection by transmission electron microscope (TEM). As shown in Fig. 2A–D, *PmAP2- $\beta$*  was accumulating around the plasma membrane of YHV-infected shrimp hemocytes. In addition, clusters of *PmAP2- $\beta$* , resembling a sac, were also observed in Fig. 2B,C. Presumably, these *PmAP2- $\beta$*  clusters may contain YHV inside.

**Effect of *PmAP2- $\beta$*  silencing on the Toll, the Imd and the JAK/STAT signaling pathways during YHV infection.** As shown in Fig. 3A,B, YHV infection significantly enhanced the transcription of *PmSpätzle* and myeloid differentiation factor 88 (MyD88) in the Toll pathway. *PmSpätzle* was increased by 12, 16, 7, 10, 10, 3 -fold at 6, 12, 18, 24, 30 and 36 hpi, respectively, while *PmMyD88* gradually increased and reached the highest level (sixfold) at 18 hpi. This suggested that the Toll signaling pathway responded to YHV infection. Notably, expression of *PmDorsal* in YHV-challenged shrimp remained at a similar level, compared with that in non-infected shrimp (Fig. 3C).

Next, the RNA interference experiment was carried out in order to investigate the influence of *PmAP2- $\beta$*  on signaling pathways and other immune-related genes during YHV infection. In previous research, we have shown that *PmAP2- $\beta$*  transcript can be efficiently suppressed by *PmAP2- $\beta$*  dsRNA<sup>7</sup>. Interestingly, expression of *PmSpätzle* in *PmAP2- $\beta$*  silenced shrimp challenged with YHV was highly up-regulated by 31- and 33-fold

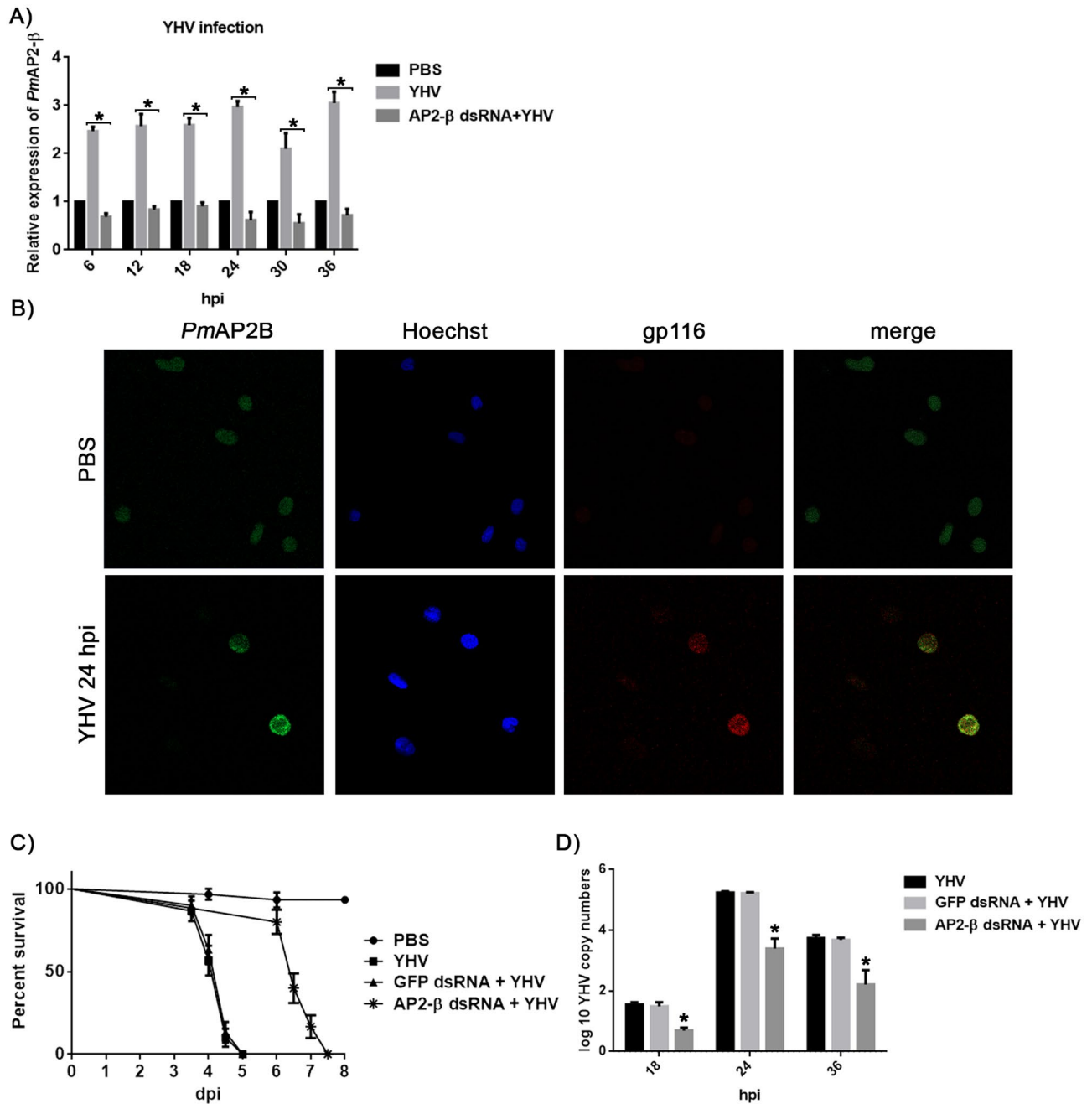


**Figure 1.** Expression of *PmAP2-β* and effect of *PmAP2-β* silencing on YHV infection. (A) The relative transcription levels of *PmAP2-β* during YHV infection. The mRNA expression levels of *PmAP2-β* were analyzed by Quantitative Real-time RT-PCR. The experiment was carried out in triplicate. (B) Expressions of *PmAP2-β* (green) and gp116 (red) in the hemocytes of unchallenged and YHV-challenged shrimp were observed by confocal laser scanning microscopy. Secondary antibodies conjugated with Alexa Fluor 488 (green) and Alexa Fluor 568 (red) were used to probe anti-AP2-β and gp116 antibodies, respectively, while nuclei were stained in blue. (C) Effect of *PmAP2-β* silencing on cumulative mortality caused by YHV. Shrimp were injected with either 150 mM NaCl or 10 μg GFP dsRNA per 1 g of shrimp or 10 μg *PmAP2-β* dsRNA per 1 g of shrimp at 24 h prior to YHV challenge. The cumulative mortality was recorded every 12 h after YHV injection. Each group contains 10 shrimps. The experiment was carried out in triplicate. (D) Determination of YHV copy number in *PmAP2-β* knockdown shrimp. Shrimp were divided into three groups and injected with either 150 mM NaCl, GFP dsRNA (10 μg/g shrimp), *PmAP2-β* dsRNA (10 μg/g shrimp). Shrimp hemocytes were collected at 6, 12, 18, 24, 30 and 36 h after YHV injection for YHV copy number determination. The data are shown as the mean ± standard deviation. An asterisk represents significant differences from control group ( $p < 0.05$ ). The experiment was carried out in triplicate.

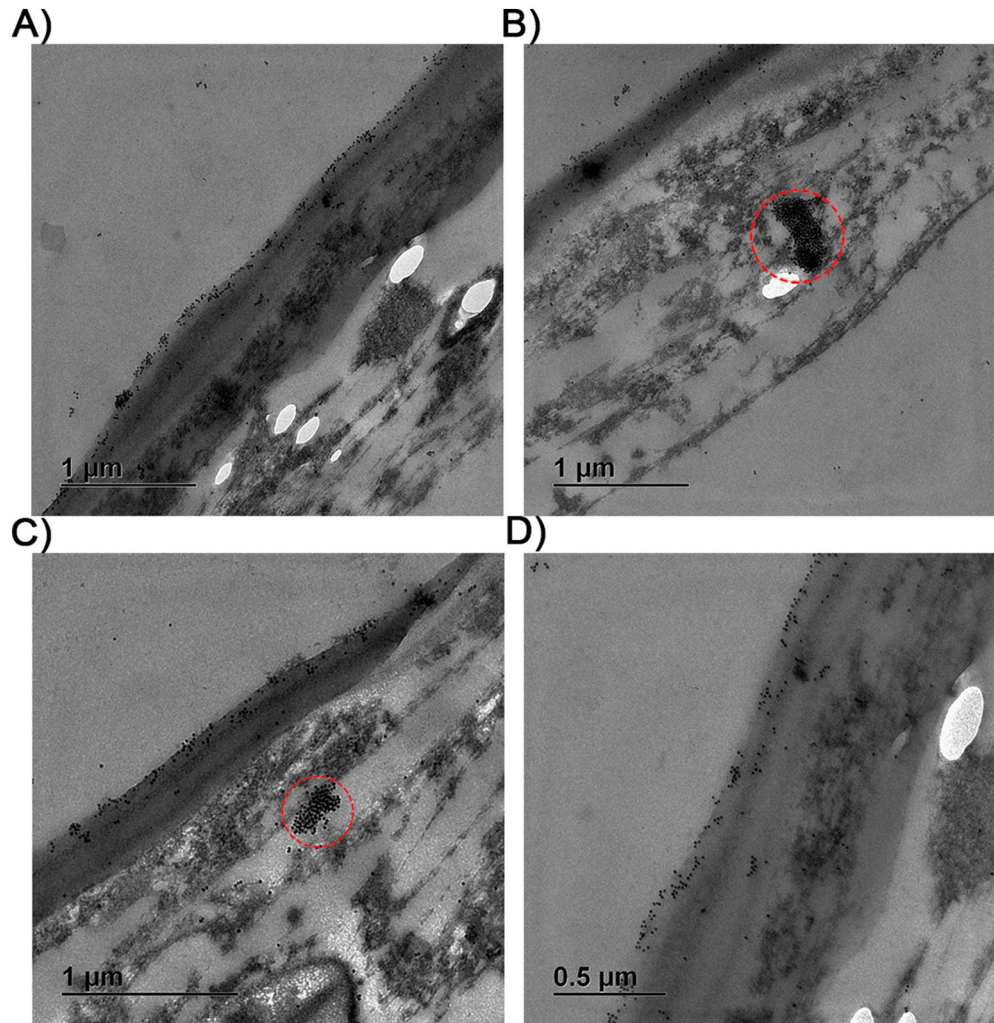


**Figure 2.** Visualization of *PmAP2-β* in YHV-infected hemocytes cell by TEM. *PmAP2-β* was detected by a 10 nm gold-conjugated anti-AP-2β antibody. Red circles show clusters of *PmAP2-β* form as a sac.

at 6 and 12 hpi, compared with non-infected shrimp (Fig. 3A). In addition, *PmAP2-β* silencing increased the expression of *PmMyD88* at 6, 18, 30 and 36 hpi (Fig. 3B), as well as *PmDorsal* at 6 and 12 hpi (Fig. 3C). Clearly, *PmAP2-β* mediates the Toll signaling pathway during YHV infection.

On the contrary, YHV infection only induced the expression of *PmRelish*, representing the Imd pathway, by threefold at 18 hpi, and *PmAP2-β* silenced shrimp did not show significant changes in *PmRelish* expression during YHV infection, except at 12 hpi (Fig. 3D). It is likely that the Imd pathway may not play an essential role in response to YHV infection.

In addition, the role of the JAK/STAT signaling pathway during YHV infection was investigated by measuring the transcription levels of *PmDOME*, *PmJAK* and *PmSTAT*. Figure 4A showed that YHV-challenged shrimp have a similar expression of *PmDOME*, compared with that in non-infected shrimp. Meanwhile, *PmJAK* was mostly down-regulated during YHV infection (Fig. 4B), while *PmSTAT* expression remained unchanged upon YHV infection, except at 24 and 36 hpi, at which *PmSTAT* was up-regulated around threefold (Fig. 4C). Silencing of *PmAP2-β* increased expression of *PmDOME* in YHV-challenged shrimp by fourfold at 24 hpi (Fig. 4A) and caused an up-regulation of *PmSTAT* by eightfold at 6 hpi and by approximately fourfold at 18, 30 and 36 hpi (Fig. 4C), in comparison with non-challenged shrimp. This result indicated that *PmAP2-β* might be associated with *PmSTAT* activation.

**Effect of *PmAP2-β* silencing on the expression of antimicrobial peptides during YHV infection.** In this work, we investigated the influence of *PmAP2-β* knockdown on the expression of ALFPm3, CrustinPm1, CrustinPm7, PEN3 and PEN5. Figure 5A showed that ALFPm3 was highly up-regulated by 16, 15, 30, 24, 3, and 25-fold at 6, 12, 18, 24, 30 and 36 h after YHV infection, respectively. CrustinPm1 was increased by threefold at 6 h upon YHV infection (Fig. 5B), while PEN3 was up-regulated at the highest level at 18 hpi (Fig. 5D). In contrast, CrustinPm7 and PEN5 seemed to give minimal response to YHV infection (Fig. 5C,E).

Silencing of *PmAP2-β* significantly increased ALFPm3 transcripts by 47, 55, 34, 58, 79, 12-fold at 6, 12, 18, 24, 30 and 36 hpi (Fig. 5A). Similarly, knockdown of *PmAP2-β* enhanced CrustinPm1 transcription level by 4,

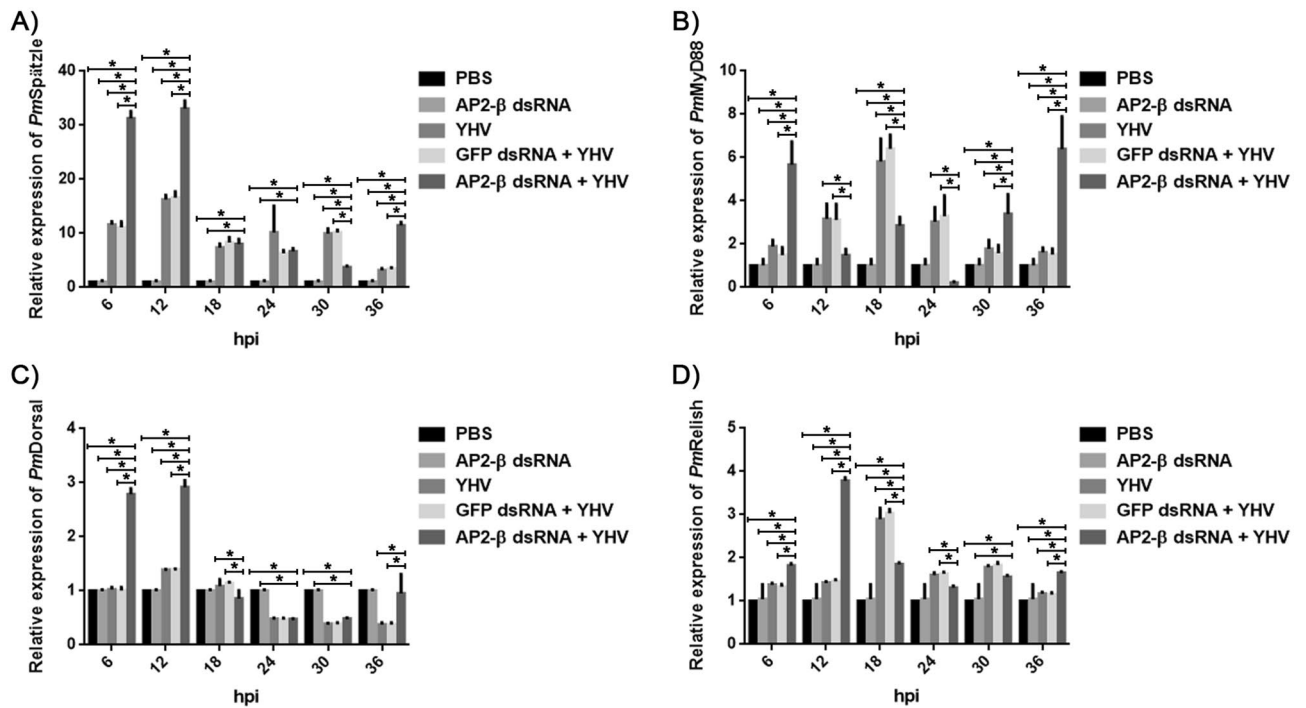


**Figure 3.** Effect of *PmAP2-β* silencing on the Toll and the Imd signaling pathways during YHV infection. Shrimp were double injected with either 150 mM NaCl, GFP dsRNA (10 µg/g shrimp) and *PmAP2-β* dsRNA (10 µg/g shrimp). After YHV injection, shrimp hemocytes were collected at 6, 12, 18, 24, 30, 36 h for qRT-PCR analysis of the transcription levels of *PmSpätzle* (A), *PmMyD88* (B), *PmDorsal* (C) and *PmRelish* (D). The data are shown as the mean ± standard deviation. An asterisk represents significant differences from control group ( $p < 0.05$ ). The experiment was carried out in triplicate.

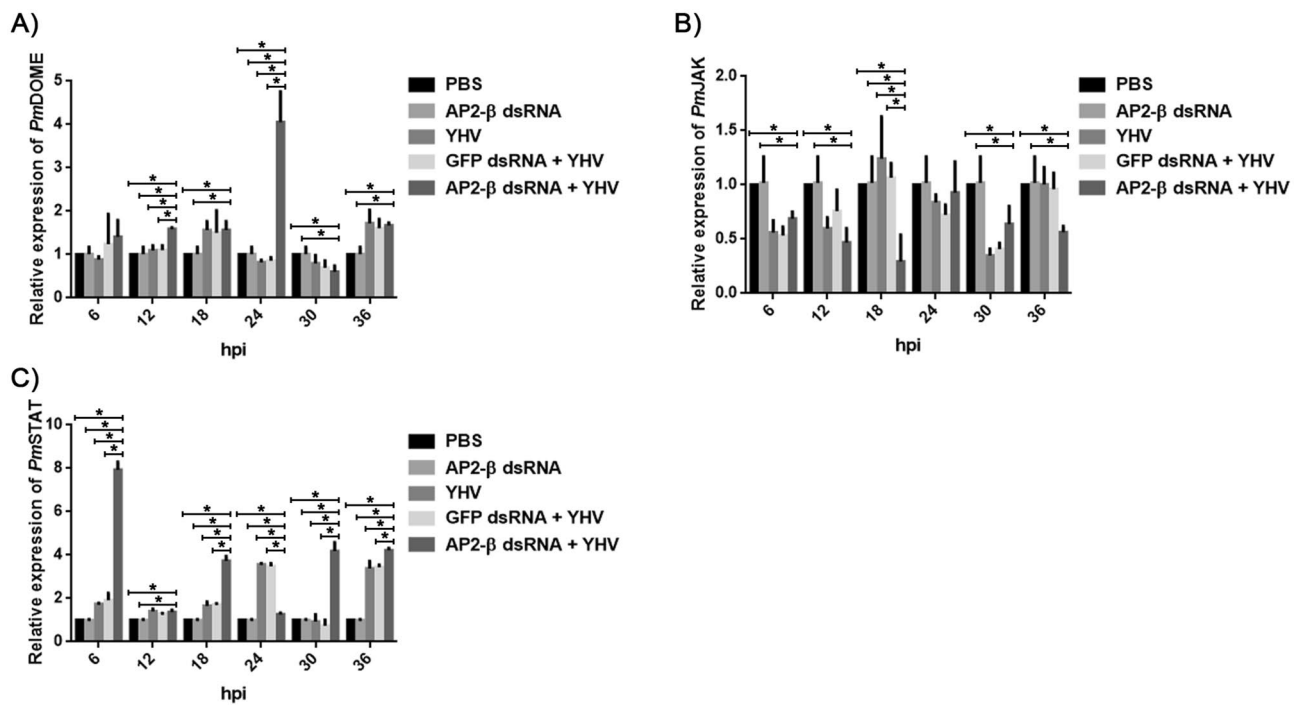


**Figure 4.** Effect of *PmAP2-β* silencing on the JAK/STAT pathways during YHV infection. *PmAP2-β* knockdown was carried out as described in "Methods". The transcription levels of *PmDOME* (A), *PmJAK* (B) and *PmSTAT* (C) at 6, 12, 18, 24, 30, 36 h after YHV infection were determined by qRT-PCR. The data are shown as the mean ± standard deviation. An asterisk represents significant differences from control group ( $p < 0.05$ ). The experiment was carried out in triplicate.

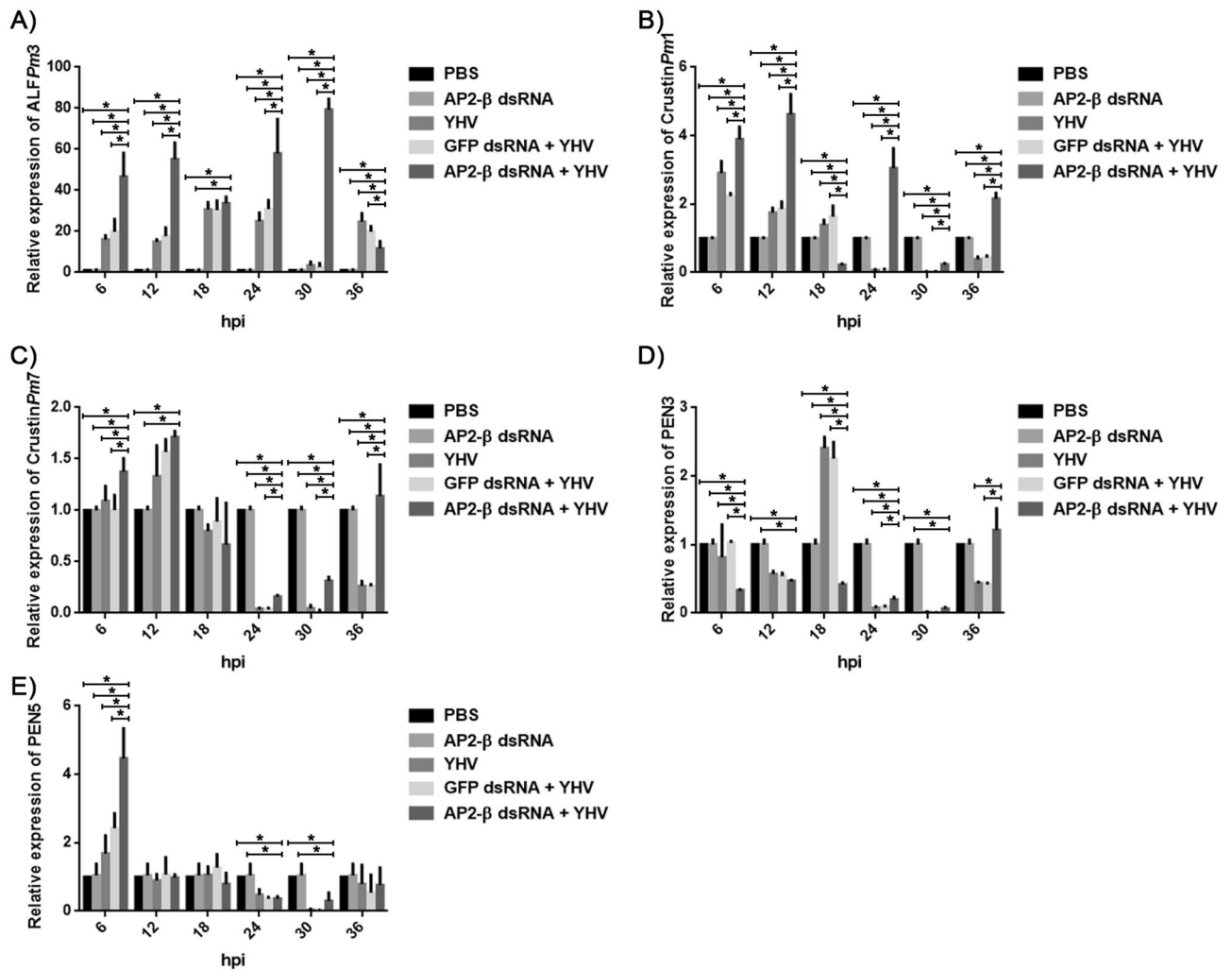


**Figure 5.** Determination of the mRNA transcription levels of antimicrobial peptides under influence of *PmAP2-β* knockdown during YHV infection. *ALFPm3* (A), *CrustinPm1* (B), *CrustinPm7* (C), *PEN3* (D) and *PEN5* (E) transcripts of *PmAP2-β*-silenced shrimp challenged by YHV at 6, 12, 18, 24, 30, 36 h were quantified by qRT-PCR and compared with those in unchallenged *PmAP2-β*-silenced, YHV-challenged, and YHV-challenged + GFP knockdown shrimp.

5 and threefold at 6, 12 and 24 h post-YHV infection (Fig. 5B). It is worth noting that expression of *PEN5* in *PmAP2-β* silenced shrimp was also increased by 4.5-fold at 6 h after YHV challenge (Fig. 5E), while *PmAP2-β* silencing did not enhance the expression of *CrustinPm7* and *PEN3* (< twofold) (Fig. 5C,D). Clearly, *ALFPm3* and *CrustinPm1* play an important role during YHV infection and their expressions were influenced by *PmAP2-β*.

***ALFPm3* and *crustinPm1* are responsible for defence against YHV.** Roles of *ALFPm3* and *CrustinPm1* against YHV were further investigated. Either *ALFPm3* or *CrustinPm1* or both *ALFPm3* and *CrustinPm1* were knocked down using *ALFPm3* dsRNA and/or *CrustinPm1* dsRNA of 1 µg per 1 g shrimp as described in “Methods”. Figure 6A–C showed that *ALFPm3* and *CrustinPm1* were successfully knocked down. Silencing of either *ALFPm3* or *CrustinPm1* alone did not alter shrimp’s survival rate upon YHV infection (Fig. 6D). However, knockdown of both *ALFPm3* or *CrustinPm1* significantly reduced survival percentage at day 2 and 3 post-YHV infection. It is likely that *ALFPm3* and *CrustinPm1* covered for each other in a defence against YHV.

## Discussion

Clathrin-mediated endocytosis plays an essential role in YHV entry into shrimp cells<sup>4,5</sup>. In this work, we studied the effects of *PmAP2-β* silencing on gene expression and shrimp mortality during YHV infection. *PmAP2-β* is a large subunit 2β of the AP-2 complex, which interacts with clathrin. Previously, *PmAP2-β* has been characterized and was shown to play a role during WSSV infection<sup>7</sup>.

In this work, *PmAP2-β* was continuously up-regulated more than twofold during YHV infection (Fig. 1A). In addition, immunofluorescence showed that the level of *PmAP2-β* protein was also increased in YHV-challenged hemocyte cells, compared with non-infected cells (Fig. 1B). Figure 2 illustrated that clusters of *PmAP2-β* located

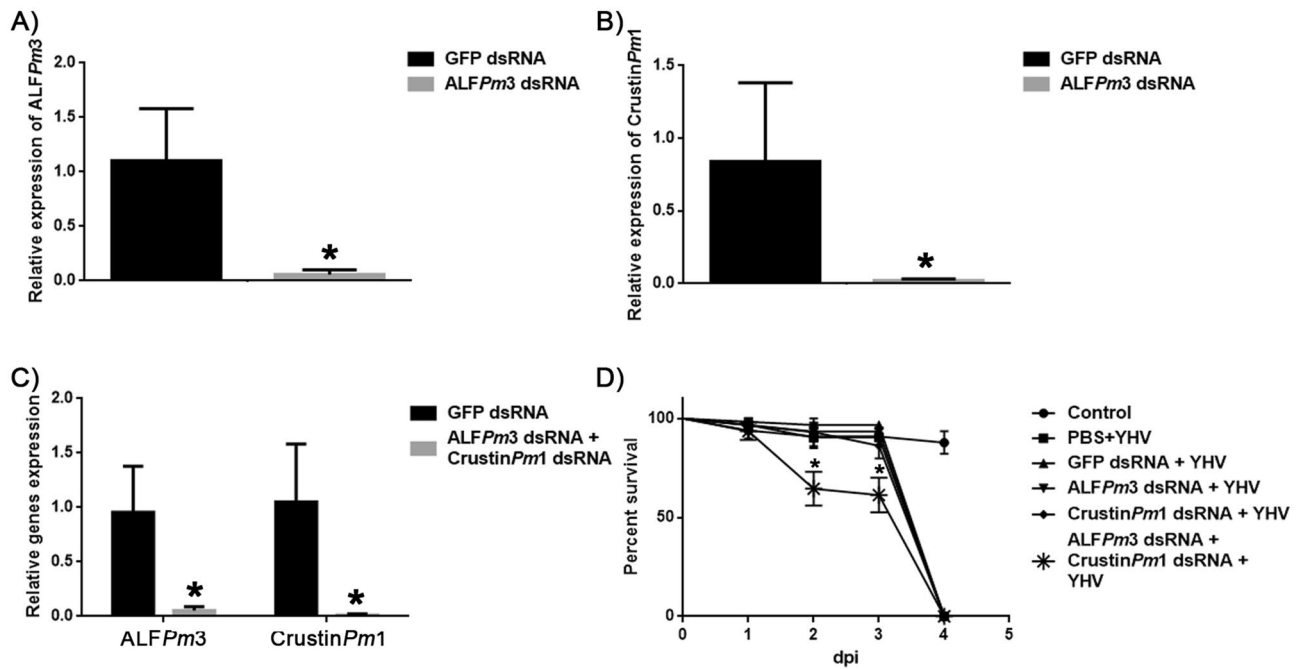


**Figure 6.** Effect of ALFPm3 and CrustinPm1 knockdown during YHV infection. Determination of ALFPm3 and CrustinPm1 transcript level in *P. monodon* hemocytes after shrimp were double injected with either 1  $\mu$ g of ALFPm3 dsRNA per 1 g shrimp (A) or 1  $\mu$ g of CrustinPm1 dsRNA per 1 g shrimp (B) or both (C). (D) Percent survival of ALFPm3 or CrustinPm1 knockdown shrimp upon YHV infection. Shrimp were divided into 6 groups, including PBS (control), YHV-challenged, YHV-challenged + GFP knockdown, YHV-challenged + ALFPm3 knockdown, YHV-challenged + CrustinPm1 knockdown and YHV-challenged + ALFPm3/CrustinPm1 knockdown. Each group contained 10 shrimps and the experiment was carried out in triplicate.

at the plasma membrane of YHV-infected shrimp cells and the sac structures of PmAP2- $\beta$ , found in the cytoplasm, may contain the virus inside. Knockdown of PmAP2- $\beta$  gave rise to a delay of shrimp mortality (Fig. 1C), as well as a reduction in YHV copy number (Fig. 1D). Clearly, silencing of PmAP2- $\beta$  disrupted YHV propagation. This may be a result of lower number of YHV entering shrimp cells via clathrin-mediated endocytosis or the silencing of PmAP2- $\beta$  triggering shrimp immune responses.

In *Drosophila*, Spätzle has been characterized as the cytokine-like molecule that binds to Toll receptor, resulting in signaling cascade through MyD88 and transcription factor Dorsal<sup>29,30</sup>. In this work, the transcription of PmSpätzle and PmMyD88 was up-regulated during YHV infection (Fig. 3A,B), suggesting that YHV activated the Toll pathway. Silencing PmAP2- $\beta$  dramatically increased PmSpätzle by 31- and 33-fold at 6 and 12 h after YHV challenge (Fig. 3A) and also enhanced PmMyD88 and PmDorsal expression levels (Fig. 3B,C). In unchallenged shrimp, PmAP2- $\beta$  knockdown did not affect PmSpätzle, PmMyD88 and PmDorsal expression, however, PmAP2- $\beta$  silenced shrimp exhibited significantly higher expression of these genes during YHV infection, compared with YHV-challenged normal shrimp. This indicated that PmAP2- $\beta$  may have an influence on the Toll pathway during YHV infection.

Depletion of PmAP2- $\beta$  seemed to amplify cellular response of the Toll signaling pathway toward YHV infection. In general, endocytosis mediates receptor signaling by (1) controlling the number of receptors present on the plasma membrane for binding extracellular ligands (2) degradation or recycling of internalized receptors modulates the strength and specificity of signal transmission (3) endosomes play a part in intracellular signaling<sup>31–33</sup>. During *Drosophila* embryogenesis, Toll signaling was suggested to occur from the endosome rather than on the plasma membrane<sup>34</sup>. In *P. monodon*, silencing of early endosome antigen 1 (EEA1) protein (PmEEA1), involving in early endosome fusion, caused a delay in shrimp mortality due to YHV infection<sup>35</sup>. Similar results were observed in YHV-challenged shrimp with either PmRab7 or PmRab11 suppression<sup>6,36</sup>. These suggested that endosome trafficking plays an important role during YHV infection. It is possible that lack of PmAP2- $\beta$  may impair clathrin-mediated endocytosis, resulting in alteration of signaling. It was previously reported that clathrin and dynamin-deficient cells showed enhanced activation of canonical NF- $\kappa$ B signaling<sup>25</sup>.

Regarding the Imd signaling pathway, PmRelish expression did not increase significantly during YHV infection and PmAP2- $\beta$ -deficiency seemed not to influence PmRelish transcript (Fig. 3D). This implied that the Imd pathway may not substantially contribute to YHV infection and PmAP2- $\beta$  deficiency did not affect the Imd signaling. Somehow, it was previously reported that PmRelish silencing made the shrimp more susceptible to YHV<sup>37</sup>. In *Drosophila*, the Imd pathway regulates immune genes against Gram-negative bacteria<sup>38</sup> and also possesses antiviral function<sup>39,40</sup>. In Chinese white shrimp *Fenneropenaeus chinensis*, FcIMD was up-regulated upon WSSV challenge, suggesting that the Imd signaling pathway was involved in antiviral innate immunity of shrimp. It was

reported that knockdown of Relish affected the activity of phenoloxidase (PO) and superoxide dismutase (SOD), and total hemocyte count (THC) after WSSV or *Vibrio alginolyticus* infection in crab *Scylla paramamosain*<sup>41</sup>.

Based on *PmDOME*, *PmJAK* and *PmSTAT* expression, the JAK/STAT did not promptly respond to YHV infection at an early stage, when only *PmSTAT* was up-regulated around threefold at 24 and 36 hpi (Fig. 4). However, under the suppression of *PmAP2-β*, the *PmSTAT* transcript significantly increased by eightfold at 6 hpi and by fourfold at 18, 30 and 36 hpi, in response to YHV (Fig. 4C). Devergne and colleagues reported that, in *Drosophila*, recruitment and trafficking of the clathrin-AP complexes into endocytic vesicles towards the lysosome could enhance the JAK/STAT signaling<sup>21</sup>. In contrast, Vidal and co-workers suggested that endocytic trafficking acts as a negative regulator of JAK/STAT signaling in *Drosophila*<sup>42</sup>. We postulated that knockdown of *PmAP2-β* may disrupt clathrin-dependent endocytosis and signaling from endocytic mechanisms, resulting in an increased expression of *PmSTAT*. It is possible that in *P. monodon*, endocytic mechanisms modulate the JAK/STAT signaling negatively.

Regulation of signaling pathways could alter the expression level of antimicrobial peptides (AMPs). In Kuruma shrimp *Marsupenaeus japonicus*, Gram-positive and Gram-negative bacteria can activate the Toll pathway by their pathogen-associated molecular patterns (PAMPs) directly binding to Toll-like receptors, enhancing the expression of AMPs such as ALF-B1, ALF-C2, CruI-1 and CruI-3<sup>43</sup>. Furthermore, injection of activated *PmSpätzle* enhanced transcription levels of ALFPm3, crustinPm1, crustinPm7 and penaeidin3 in black tiger shrimp<sup>44</sup>. The recombinant Spätzle-like protein from Chinese shrimp, *Fenneropenaeus chinensis* could also increase crustin 2 expression in crayfish<sup>45</sup>.

Silencing of *PmRelish* shrimp suppressed the expression level of penaeidin5, but did not affect ALFPm3, crustinPm1 and penaeidin3 expression levels<sup>37</sup>. Knockdown of *IMD* in *Procambarus clarkii* inhibited the expression of *Cru1* and 2, *ALF 1* and 2 and *Lys1* in red swamp crayfish challenged with *Vibrio anguillarum*<sup>46</sup>. In crab *S. paramamosain*, Relish knockdown caused a downregulation of immune genes such as JAK, crustin and phenoloxidase<sup>41</sup>.

Regarding the JAK/STAT, knockdown of suppressor of cytokine signaling 2 (SOCS2) increased ALF-C1, C2 and D1, and Crustin I expression levels upon *V. anguillarum* challenge<sup>47</sup>. Meanwhile, injection of recombinant SOCS2 reduced STAT phosphorylation and inhibited STAT translocation into the nucleus, resulting in a decline in the AMP expression.

Since *PmAP2-β* seemed to regulate the signaling cascades, effects of *PmAP2-β* silencing on AMP expression have been investigated. In general, ALFs showed broad antimicrobial activity against Gram-positive and Gram-negative bacteria, fungi and viruses, while crustins mainly exhibited antibacterial activity and penaeidins mostly functioned against bacteria and fungi. Previously, a suppression subtractive hybridization (SSH) study reported apparently up-regulated AMPs, including ALFPm6 and crustinPm1 in response to YHV infection<sup>48</sup>. Figure 5 showed that among five AMPs (ALFPm3, CrustinPm1, CrustinPm3, PEN3 and PEN5), ALFPm3 was the most active AMPs against YHV. *PmAP2-β* depleted shrimp showed a significant increase in both ALFPm3 and CrustinPm1 expressions during YHV infection, compared with normal shrimp challenged with YHV. We postulated that *PmAP2-β* depletion amplified the Toll signaling during YHV infection, resulting in elevated levels of ALFPm3 and CrustinPm1. Consistent with this, *PmAP2-β*-deprived shrimp were more resistant to YHV, than normal shrimp (Fig. 2C). In addition, ALFPm3 and CrustinPm1 silenced shrimp had lower survival rate on days 2 and 3, compared with normal shrimp infected by YHV (Fig. 6D). This indicated that ALFPm3 and CrustinPm1 are important in defence against YHV. Previous research demonstrated that crustinPm1 was found in the granule-containing hemocytes targeted by YHV<sup>49</sup>.

In conclusion, this research suggested that clathrin-mediated endocytosis not only functions as an entry route for YHV but also plays a role in regulating the intracellular signals. *PmAP2-β* depletion stimulated the Toll signaling, resulting in elevated levels of ALFPm3 and CrustinPm1 during YHV infection. Both ALFPm3 and CrustinPm1 are essential antimicrobial peptides, acting against YHV.

## Methods

**Shrimp.** Healthy black tiger shrimp, *P. monodon*, of about 3.23 ± 0.15 g bodyweight, were from Charoen Pokphand Farm in Chanthaburi Province, Thailand. They were acclimated in laboratory tanks (120 L) at ambient temperature (28 ± 4 °C) and maintained in aerated water with a salinity of 20 ppt for at least 1 week before starting the experiments.

**YHV stock preparation.** YHV stock was prepared as described in previous study<sup>4</sup>. Briefly, hemolymph was drained from YHV-infected moribund shrimp by 1 ml syringe containing an equal volume of modified Alsever solution (MAS: 27 mM sodium citrate, 336 mM NaCl, 115 mM glucose, 9 mM EDTA, pH 7.0). Hemocytes were removed by centrifugation at 1000×g for 10 min at 4 °C. The supernatant was filtered with 0.45 μm MILLEX-HP filter unit and centrifuged at 30,000×g for 30 min at 4 °C. The pellet was washed twice with TN buffer (50 mM Tris-HCl, pH 7.4 and 100 mM NaCl), then, aliquoted and kept at -80 °C until use. YHV copy number was quantified by qRT-PCR using a specific primer pair for YHV genome (YHV-141-F and YHV-206-R in Table S1)<sup>50</sup>.

**Expression of *PmAP2-β* during YHV infection.** Healthy shrimp were separated into two groups, each of which consists of nine individuals, and was injected with either 50 μl of PBS or YHV (500,000 copies). Hemolymph was withdrawn from the abdomen connecting to the first pleopod using a 26-gauge needle and a 1 ml syringe containing an equal volume of ice-cold MAS solution. Each sample contains hemolymph from 3 shrimps (approximately 200 μl of hemolymph per individual). Hemocytes were pelleted by centrifugation at 800×g for 10 min at 4 °C. Total RNA was extracted by FavorPrep Tissue Total RNA mini kit (Favogen) and followed by cDNA synthesis using RevertAid First Strand cDNA Synthesis kit (ThermoFisher). *PmAP2-β* transcription level was

quantified by qRT-PCR using specific primers for *PmAP2-β* (Supplementary Information, Table S1). Elongation factor-1 alpha (EF-1α) gene was used as an internal control. The experiment was performed in triplicate. Mathematical model was used to analyze the threshold cycle ( $C_T$ )<sup>51</sup>. Statistical analysis was done using the one-way ANOVA followed by a post hoc test. The result differences were considered significant at  $p < 0.05$  (\*).

Comparative  $C_T$  method was employed to compare the gene expression in two different samples. The fold change of gene expression was calculated as follows:

$$\text{Fold change} = 2^{-\Delta\Delta C_T}$$

$$\Delta\Delta C_T = [(C_T \text{ gene of interest} - C_T \text{ internal control}) \text{ sample A} \\ - (C_T \text{ gene of interest} - C_T \text{ internal control}) \text{ sample B}]$$

**Immunofluorescence confocal microscopy.** Either diluted YHV stock solution (approximately 10,000 copies per  $\mu\text{l}$ ) or 150 mM NaCl was injected into shrimp. The hemolymph was collected at 24 h post-injection and mixed in an equal volume of 4% paraformaldehyde in PBS. Hemocytes were collected by centrifugation ( $800\times g$  for 10 min at 4 °C), washed 3 times with PBS and fixed on microscope slides. Hemocytes were incubated with 0.1% Triton X-100 in PBS for 5 min and washed 3 times with PBS. Purified rabbit anti-AP2- $\beta$  (Abcam) polyclonal IgG antibody in 1:50 dilution in PBSF (PBS with 1% (v/v) FBS) was used to probe *PmAP2-β*, followed by Alexa Fluor 488 goat anti-rabbit IgG antibody (Invitrogen), diluted 1:500. YHV was detected by monoclonal IgG antibody specific to gp116<sup>52</sup>, diluted 1:50 in PBSF, followed by a 1:1000 dilution of Alexa Fluor 568 goat anti-mouse IgG antibody (Invitrogen). Nuclei were stained with 1:1,000 dilution of Hoechst (ThermoFisher) in PBS. The microscope slides containing the stained and fixed hemocytes were then coated by ProLong Gold (Invitrogen) and kept in the dark at 4 °C until they were observed by a confocal fluorescence microscopy.

**Visualization of *PmAP2-β* by TEM.** Shrimp (3–5 g) were injected by YHV of approximately 10,000 copy numbers and gill tissues were then collected at 30 hpi and immediately fixed by 4% paraformaldehyde. Fixed tissues were then washed three times by ice-cold PBS and followed by the manufacturer's protocol for embedding by LR White Embedding Medium (EMS). The embedded gills were cut into ultrathin sections (60–70 nm) and placed on a Formvar-supported nickel grid. The grids were incubated with 5% BSA in PBS for 1 h. A 10 nm gold particle was conjugated to primary AP-2 $\beta$  antibody (Abcam) using InnovaCoat Gold Conjugation kit. The gold conjugated antibody was diluted 1:50 by 1% BSA in PBS. The grids were incubated with diluted gold conjugated antibody solution at 4 °C overnight and stained with uranyl acetate solution for 5 min, followed by Reynolds lead citrate solutions for 2 min, and observed using Transmission Electron Microscope Libra 120 Plus (ZEISS) at the Microscopy Unit of IBT-UNAM.

**Mortality assay of *PmAP2-β* silencing shrimp upon YHV infection.** Double-strand RNA of *PmAP2-β* and GFP were prepared as described previously<sup>7</sup>. In brief, the PCR products (*PmAP2-β* and GFP) were amplified separately by specific primers (Supplementary Information, Table S1) with the following conditions: 94 °C for 3 min (denaturation), followed by 40 cycles of 94 °C for 30 s, 55 °C for 30 s and 72 °C for 30 s and a final extension at 72 °C for 10 min. The two PCR product templates were in vitro transcribed using the T7 RiboMAX System (Promega) to produce two complementary single-stranded RNAs. Then, RQ1 RNase-free DNase was added and incubated at 37 °C for 1 h and the single-stranded RNAs were then purified by standard phenol-chloroform extraction. To generate dsRNA, equal amounts of each of the complementary single-stranded RNAs were mixed, incubated at 70 °C for 10 min, and slowly cooled down at room temperature. The quality and quantity of *PmAP2-β* dsRNA and GFP dsRNA were analyzed by 1% agarose gel electrophoresis and absorbance at 260 nm, respectively.

To study the effect of *PmAP2-β* silencing, black tiger shrimp were divided into four groups, each of which consisted of 10 individuals and were injected with either PBS (group 1, control), PBS + YHV (group 2), 10  $\mu\text{g}$  of *PmAP2-β* dsRNA per 1 g of shrimp + YHV (group 3) and 10  $\mu\text{g}$  of GFP dsRNA per 1 g of shrimp + YHV (group 4). In this experiment, a diluted YHV solution containing approximately 10,000 copies per  $\mu\text{l}$  was injected into shrimp at 24 h after PBS or dsRNA injection. The mortality was recorded every 12 hpi up to 8 days. This experiment was carried out in triplicate. Data were analyzed using GraphPad Prism 6 plot, and presented as percent survival with the  $p$  values calculated by log-rank test.

**Influence of *PmAP2-β* silencing on YHV copy numbers and *P. monodon* immune related genes during YHV infection.** Shrimp hemocytes were collected at different timepoints (6, 12, 18, 24, 30 and 36 h-post injection) from *P. monodon* treated with YHV, GFP dsRNA + YHV and *PmAP2-β* dsRNA + YHV. Total RNA extraction and cDNA synthesis were performed as described previously. *P. monodon* immune related genes and YHV copy number were quantified by quantitative RT-PCR using specific primers as shown in Supplementary Information, Table S1. Elongation factor-1 alpha (EF-1α) gene was used as an internal control. The experiment was performed in triplicate and the mathematical model was used to analyze the threshold cycle ( $C_T$ ). Statistical analysis was done using the one-way ANOVA followed by a post hoc test. The result differences were considered significant at  $p < 0.05$  (\*).

**Mortality assay of ALFPm3 and/or CrustinPm1 knockdown shrimp upon YHV infection.** The DNA amplicon templates of ALFPm3 and CrustinPm1 were amplified using primers in Supplementary Informa-

tion, Table S1 and ALFPm3 and CrustinPm1 dsRNA synthesis was performed as described above. Either ALFPm3 dsRNA or CrustinPm1 dsRNA was injected at 1 µg per 1 g of shrimp and the hemocytes were collected at 24 hpi. Total RNA and cDNA synthesis were performed as described above; and the level of ALFPm3 and CrustinPm1 transcripts were determined by qRT-PCR. In the mortality experiment, shrimp were divided into 6 groups with 10 shrimps per group as followed, Group 1: PBS (control), Group 2: YHV-challenged, Group 3: YHV-challenged + GFP dsRNA, Group 4: YHV-challenged + ALFPm3 dsRNA, Group 5: YHV-challenged + CrustinPm1 dsRNA, and Group 6: YHV-challenged + ALFPm3/CrustinPm1 dsRNAs. After YHV injection, shrimp mortality was recorded every 12 h up to 4 days. The experiment was performed in triplicate and the data were analyzed using GraphPad Prism 6 and presented as percent survival with the *p* values calculated by log-rank test.

Received: 20 January 2021; Accepted: 4 May 2021

Published online: 18 May 2021

## References

- Flegel, T. W. Special topic review: Major viral diseases of the black tiger prawn (*Penaeus monodon*) in Thailand. *World J. Microbiol. Biotechnol.* **13**, 433–442 (1997).
- Lightner, D. V., Hasson, K. W., White, B. L. & Redman, R. M. Experimental infection of western hemisphere penaeid shrimp with Asian white spot syndrome virus and Asian yellow head virus. *J. Aquat. Anim. Health* **10**, 271–281 (1998).
- Lu, Y., Tapay, L. M., Brock, J. A. & Loh, P. C. Infection of the yellowhead baculo-like virus (YBV) in two species of penaeid shrimp, *Penaeus stylirostris* (Simpson) and *Penaeus vannamei* (Boone). *J. Fish Dis.* **17**, 649–656 (1994).
- Jatuyosorn, T., Supungul, P., Tassanakajon, A. & Krusong, K. The essential role of clathrin-mediated endocytosis in yellow head virus propagation in the black tiger shrimp *Penaeus monodon*. *Dev. Comp. Immunol.* **44**, 100–110. <https://doi.org/10.1016/j.dci.2013.11.017> (2014).
- Posiri, P., Kondo, H., Hirono, I., Panyim, S. & Ongvarrasopone, C. Successful yellowhead virus infection of *Penaeus monodon* requires clathrin heavy chain. *Aquaculture* **435**, 408–487 (2015).
- Ongvarrasopone, C., Chanasakulniyom, M., Sritunyalucksana, K. & Panyim, S. Suppression of PmRab7 by dsRNA inhibits WSSV or YHV infection in shrimp. *Mar. Biotechnol. (NY)* **10**, 374–381. <https://doi.org/10.1007/s10126-007-9073-6> (2008).
- Jatuyosorn, T. *et al.* Role of clathrin assembly protein-2 beta subunit during white spot syndrome virus infection in black tiger shrimp *Penaeus monodon*. *Sci. Rep.-UK* **9**, 13489. <https://doi.org/10.1038/s41598-019-49852-0> (2019).
- Kaksonen, M. & Roux, A. Mechanisms of clathrin-mediated endocytosis. *Nat. Rev. Mol. Cell Biol.* **19**, 313–326. <https://doi.org/10.1038/nrm.2017.132> (2018).
- Pryor, P. R. & Luzio, J. P. Delivery of endocytosed membrane proteins to the lysosome. *Biochim. Biophys. Acta* **1793**, 615–624. <https://doi.org/10.1016/j.bbamcr.2008.12.022> (2009).
- Doxsey, S. J., Brodsky, F. M., Blank, G. S. & Helenius, A. Inhibition of endocytosis by anti-clathrin antibodies. *Cell* **50**, 453–463. [https://doi.org/10.1016/0092-8674\(87\)90499-5](https://doi.org/10.1016/0092-8674(87)90499-5) (1987).
- Cureton, D. K., Massol, R. H., Saffarian, S., Kirchhausen, T. L. & Whelan, S. P. Vesicular stomatitis virus enters cells through vesicles incompletely coated with clathrin that depend upon actin for internalization. *PLoS Pathog.* **5**, e1000394. <https://doi.org/10.1371/journal.ppat.1000394> (2009).
- Suzuki, T. *et al.* Sialidase activity of influenza A virus in an endocytic pathway enhances viral replication. *J. Virol.* **79**, 11705–11715. <https://doi.org/10.1128/JVI.79.18.11705-11715.2005> (2005).
- Johns, H. L., Berryman, S., Monaghan, P., Belsham, G. J. & Jackson, T. A dominant-negative mutant of rab5 inhibits infection of cells by foot-and-mouth disease virus: Implications for virus entry. *J. Virol.* **83**, 6247–6256. <https://doi.org/10.1128/JVI.02460-08> (2009).
- Blanchard, E. *et al.* Hepatitis C virus entry depends on clathrin-mediated endocytosis. *J. Virol.* **80**, 6964–6972. <https://doi.org/10.1128/JVI.00024-06> (2006).
- Wang, X. F., Liu, Q. H., Wu, Y. & Huang, J. *Litopenaeus vannamei* clathrin coat AP17 involved in white spot syndrome virus infection. *Fish Shellfish Immunol.* **52**, 309–316. <https://doi.org/10.1016/j.fsi.2016.03.007> (2016).
- Huang, J., Li, F., Wu, J. & Yang, F. White spot syndrome virus enters crayfish hematopoietic tissue cells via clathrin-mediated endocytosis. *Virology* **486**, 35–43. <https://doi.org/10.1016/j.virol.2015.08.034> (2015).
- Calebiro, D., Nikolaev, V. O., Persani, L. & Lohse, M. J. Signaling by internalized G-protein-coupled receptors. *Trends Pharmacol. Sci.* **31**, 221–228. <https://doi.org/10.1016/j.tips.2010.02.002> (2010).
- Yap, C. C. & Winckler, B. Harnessing the power of the endosome to regulate neural development. *Neuron* **74**, 440–451. <https://doi.org/10.1016/j.neuron.2012.04.015> (2012).
- Sadowski, L., Pilecka, I. & Miaczynska, M. Signaling from endosomes: Location makes a difference. *Exp. Cell Res.* **315**, 1601–1609. <https://doi.org/10.1016/j.yexcr.2008.09.021> (2009).
- Vaccari, T., Lu, H., Kanwar, R., Fortini, M. E. & Bilder, D. Endosomal entry regulates Notch receptor activation in *Drosophila melanogaster*. *J. Cell Biol.* **180**, 755–762. <https://doi.org/10.1083/jcb.200708127> (2008).
- Devergne, O., Ghiglione, C. & Noselli, S. The endocytic control of JAK/STAT signalling in *Drosophila*. *J. Cell Sci.* **120**, 3457–3464. <https://doi.org/10.1242/jcs.005926> (2007).
- Marchetti, M. *et al.* Stat-mediated signaling induced by type I and type II interferons (IFNs) is differentially controlled through lipid microdomain association and clathrin-dependent endocytosis of IFN receptors. *Mol. Biol. Cell* **17**, 2896–2909. <https://doi.org/10.1091/mbc.E06-01-0076> (2006).
- Munthe, E., Raiborg, C., Stenmark, H. & Wenzel, E. M. Clathrin regulates Wnt/beta-catenin signaling by affecting Golgi to plasma membrane transport of transmembrane proteins. *J. Cell Sci.* <https://doi.org/10.1242/jcs.244467> (2020).
- Husebye, H. *et al.* Endocytic pathways regulate Toll-like receptor 4 signaling and link innate and adaptive immunity. *EMBO J.* **25**, 683–692. <https://doi.org/10.1038/sj.emboj.7600991> (2006).
- Maksymowicz, M., Miaczynska, M. & Banach-Orłowska, M. Clathrin- and dynamin-dependent endocytosis limits canonical NF-κB signaling triggered by lymphotoxin beta receptor. *Cell Commun. Signal* **18**, 176. <https://doi.org/10.1186/s12964-020-00664-0> (2020).
- Kamsaeng, P., Tassanakajon, A. & Somboonwivat, K. Regulation of antilipopolysaccharide factors, ALFPm3 and ALFPm6, in *Penaeus monodon*. *Sci. Rep.-UK* **7**, 12694. <https://doi.org/10.1038/s41598-017-12137-5> (2017).
- Arayamethakorn, S., Supungul, P., Tassanakajon, A. & Krusong, K. Corrigendum to “Characterization of molecular properties and regulatory pathways of CrustinPm1 and CrustinPm7 from the black tiger shrimp *Penaeus monodon*” [Dev. Comp. Immunol. **67** (2017) 18–29]. *Dev. Comp. Immunol.* <https://doi.org/10.1016/j.dci.2017.05.001> (2017).

28. Visetnan, S. *et al.* YHV-responsive gene expression under the influence of *PmRelish* regulation. *Fish Shellfish Immunol.* **47**, 572–581. <https://doi.org/10.1016/j.fsi.2015.09.053> (2015).
29. Weber, A. N. *et al.* Binding of the *Drosophila* cytokine Spätzle to Toll is direct and establishes signaling. *Nat Immunol* **4**, 794–800. <https://doi.org/10.1038/ni955> (2003).
30. An, C., Jiang, H. & Kanost, M. R. Proteolytic activation and function of the cytokine Spätzle in the innate immune response of a lepidopteran insect, *Manduca sexta*. *FEBS J.* **277**, 148–162. <https://doi.org/10.1111/j.1742-4658.2009.07465.x> (2010).
31. Schmid, S. L. Reciprocal regulation of signaling and endocytosis: Implications for the evolving cancer cell. *J. Cell Biol.* **216**, 2623–2632. <https://doi.org/10.1083/jcb.201705017> (2017).
32. Sorkin, A. & Goh, L. K. Endocytosis and intracellular trafficking of ErbBs. *Exp. Cell Res.* **315**, 683–696. <https://doi.org/10.1016/j.yexcr.2008.07.029> (2009).
33. Budick-Harmelin, N. & Miaczynska, M. Integration of the endocytic system into the network of cellular functions. *Prog. Mol. Subcell Biol.* **57**, 39–63. [https://doi.org/10.1007/978-3-319-96704-2\\_2](https://doi.org/10.1007/978-3-319-96704-2_2) (2018).
34. Lund, V. K., DeLotto, Y. & DeLotto, R. Endocytosis is required for Toll signaling and shaping of the Dorsal/NF- $\kappa$ B morphogen gradient during *Drosophila* embryogenesis. *Proc. Natl. Acad. Sci. U S A* **107**, 18028–18033. <https://doi.org/10.1073/pnas.1009157107> (2010).
35. Posiri, P., Thongsuksangcharoen, S., Chaysri, N., Panyim, S. & Ongvarrasopone, C. *PmEEA1*, the early endosomal protein is employed by YHV for successful infection in *Penaeus monodon*. *Fish Shellfish Immunol.* **95**, 449–455. <https://doi.org/10.1016/j.fsi.2019.10.054> (2019).
36. Kongprajug, A., Panyim, S. & Ongvarrasopone, C. Suppression of *PmRab11* inhibits YHV infection in *Penaeus monodon*. *Fish Shellfish Immunol.* **66**, 433–444 (2017).
37. Visetnan, S., Supungul, P., Hirono, I., Tassanakajon, A. & Rimphanitchayakit, V. Activation of *PmRelish* from *Penaeus monodon* by yellow head virus. *Fish Shellfish Immunol.* **42**, 335–344. <https://doi.org/10.1016/j.fsi.2014.11.015> (2015).
38. Gottar, M. *et al.* The *Drosophila* immune response against Gram-negative bacteria is mediated by a peptidoglycan recognition protein. *Nature* **416**, 640–644. <https://doi.org/10.1038/nature734> (2002).
39. Costa, A., Jan, E., Sarnow, P. & Schneider, D. The Imd pathway is involved in antiviral immune responses in *Drosophila*. *PLoS ONE* **4**, e7436. <https://doi.org/10.1371/journal.pone.0007436> (2009).
40. Avadhanula, V., Weasner, B. P., Hardy, G. G., Kumar, J. P. & Hardy, R. W. A novel system for the launch of alphavirus RNA synthesis reveals a role for the Imd pathway in arthropod antiviral response. *PLoS Pathog.* **5**, e1000582. <https://doi.org/10.1371/journal.ppat.1000582> (2009).
41. Zhu, F., Sun, B. & Wang, Z. The crab Relish plays an important role in white spot syndrome virus and *Vibrio alginolyticus* infection. *Fish Shellfish Immunol.* **87**, 297–306. <https://doi.org/10.1016/j.fsi.2019.01.028> (2019).
42. Vidal, O. M., Stec, W., Bausek, N., Smythe, E. & Zeidler, M. P. Negative regulation of *Drosophila* JAK-STAT signalling by endocytic trafficking. *J. Cell Sci.* **123**, 3457–3466. <https://doi.org/10.1242/jcs.066902> (2010).
43. Sun, J. J. *et al.* Activation of Toll pathway is different between kuruma shrimp and drosophila. *Front. Immunol.* **8**, 1151. <https://doi.org/10.3389/fimmu.2017.01151> (2017).
44. Boonrawd, S. *et al.* Characterization of *PmSptzle 1* from the black tiger shrimp *Penaeus monodon*. *Fish Shellfish Immunol.* **65**, 88–95. <https://doi.org/10.1016/j.fsi.2017.04.005> (2017).
45. Shi, X. Z. *et al.* Identification and molecular characterization of a Spätzle-like protein from Chinese shrimp (*Fenneropenaeus chinensis*). *Fish Shellfish Immunol.* **27**, 610–617. <https://doi.org/10.1016/j.fsi.2009.07.005> (2009).
46. Lan, J. F. *et al.* Characterization of an immune deficiency homolog (IMD) in shrimp (*Fenneropenaeus chinensis*) and crayfish (*Procambarus clarkii*). *Dev. Comp. Immunol.* **41**, 608–617. <https://doi.org/10.1016/j.dci.2013.07.004> (2013).
47. Sun, J. J., Lan, J. F., Xu, J. D., Niu, G. J. & Wang, J. X. Suppressor of cytokine signaling 2 (SOCS2) negatively regulates the expression of antimicrobial peptides by affecting the Stat transcriptional activity in shrimp *Marsupenaeus japonicus*. *Fish Shellfish Immunol.* **56**, 473–482. <https://doi.org/10.1016/j.fsi.2016.07.037> (2016).
48. Prapavorarat, A., Pongsomboon, S. & Tassanakajon, A. Identification of genes expressed in response to yellow head virus infection in the black tiger shrimp, *Penaeus monodon*, by suppression subtractive hybridization. *Dev. Comp. Immunol.* **34**, 611–617. <https://doi.org/10.1016/j.dci.2010.01.002> (2010).
49. Havanapan, P. O., Taengchaiyaphum, S., Ketterman, A. J. & Krittanai, C. Yellow head virus infection in black tiger shrimp reveals specific interaction with granule-containing hemocytes and crustin *Pm1* as a responsive protein. *Dev. Comp. Immunol.* **54**, 126–136. <https://doi.org/10.1016/j.dci.2015.09.005> (2016).
50. Dhar, A. K., Roux, M. M. & Klimpel, K. R. Quantitative assay for measuring the Taura syndrome virus and yellow head virus load in shrimp by real-time RT-PCR using SYBR Green chemistry. *J. Virol. Methods* **104**, 69–82 (2002).
51. Pfaffl, M. W. A new mathematical model for relative quantification in real-time RT-PCR. *Nucleic Acids Res.* **29**, e45 (2001).
52. Soowannayan, C. *et al.* Detection and differentiation of yellow head complex viruses using monoclonal antibodies. *Dis. Aquat. Organ.* **57**, 193–200 (2003).

## Acknowledgements

We thank Charoen Pokphand Foods in Chanthaburi, Thailand for providing black tiger shrimp, Professor Dr. Paisarn Sithigorngul for anti-YHV antibody and Dr. Guadalupe Trinidad Zavala Padilla at UNAM for technical assistance with TEM. This work was financially supported by Thailand Research Fund RSA6180069. Additional supports came from the Genomics Research Network on Disease Resistance in Shrimp (IRN61W0001) and Chulalongkorn University through Structural and Computational Biology Research Unit and Center of Excellence for Molecular Biology and Genomics of Shrimp. We acknowledge Chulalongkorn University for supporting T.J. via the 100th Anniversary Chulalongkorn University Fund for Doctoral Scholarship, the 90th Anniversary of Chulalongkorn University Fund (Ratchadaphiseksomphot Endowment Fund), and the Overseas Research Experience Scholarship for Graduate Student from the Graduate School. Authors also acknowledge the UNAM-CIC-CIAD 2019 academic exchange program and the DGAPA PAPPIT UNAM funding program (IN215520).

## Author contributions

T.J. conducted all experiments with assistance from P.L. in shrimp culture, gene silencing experiments and qRT-PCR. P.S., A.T. and K.K. supervised T.J. R.S-M. and A. O-L. provided access to TEM and supervised T.J. on TEM experiment. K.K. designed the experiments, analyzed data and wrote the manuscript with help from T.J. All authors reviewed the results and approved the final version of the manuscript.

## Competing interests

The authors declare no competing interests.

### Additional information

**Supplementary Information** The online version contains supplementary material available at <https://doi.org/10.1038/s41598-021-89922-w>.

**Correspondence** and requests for materials should be addressed to K.K.

**Reprints and permissions information** is available at [www.nature.com/reprints](http://www.nature.com/reprints).

**Publisher's note** Springer Nature remains neutral with regard to jurisdictional claims in published maps and institutional affiliations.



**Open Access** This article is licensed under a Creative Commons Attribution 4.0 International License, which permits use, sharing, adaptation, distribution and reproduction in any medium or format, as long as you give appropriate credit to the original author(s) and the source, provide a link to the Creative Commons licence, and indicate if changes were made. The images or other third party material in this article are included in the article's Creative Commons licence, unless indicated otherwise in a credit line to the material. If material is not included in the article's Creative Commons licence and your intended use is not permitted by statutory regulation or exceeds the permitted use, you will need to obtain permission directly from the copyright holder. To view a copy of this licence, visit <http://creativecommons.org/licenses/by/4.0/>.

© The Author(s) 2021